Appl. Sci. **2015**, *5*, 1980-1991; doi:10.3390/app5041980

OPEN ACCESS

applied sciences

ISSN 2076-3417

www.mdpi.com/journal/applsci

Article

Image Hiding Scheme Based on the Atrial Fibrillation Model

Martynas Vaidelys, Jurate Ragulskiene, Pranas Ziaukas and Minvydas Ragulskis *

Research Group for Mathematical and Numerical Analysis of Dynamical Systems, Kaunas University of Technology, Studentu 50, Kaunas LT-51368, Lithuania; E-Mails: martynas.vaidelys@ktu.lt (M.V.); jurate.ragulskiene@ktu.lt (J.R.); pranas.ziaukas@ktu.edu (P.Z.)

* Author to whom correspondence should be addressed; E-Mail: minvydas.ragulskis@ktu.lt; Tel.:+370-698-22456.

Academic Editors: Chien-Hung Liu, Cheng-Chi Wang and Chih Jer Lin

Received: 29 October 2015 / Accepted: 14 December 2015 / Published: 21 December 2015

Abstract: An image communication scheme based on the atrial fibrillation (AF) model is presented in this paper. Self-organizing patterns produced by the AF model are used to hide and transmit secret visual information. A secret image is encoded into the random matrix of initial cell excitation states in the form of a dot-skeleton representation. Self-organized patterns produced by such initial cell states ensure a secure and efficient transmission of secret visual images. Procedures for digital encoding and decoding of secret images, as well as the sensitivity of the communication scheme to the perturbation of the AF model's parameters are discussed in the paper.

Keywords: pattern formation; atrial fibrillation; communication scheme

1. Introduction

Spatial self-organizing patterns (SOP) can be effectively exploited for hiding and transmitting secret digital images. A digital fingerprint image is used as the initial condition for the evolution of a pattern in a model of reaction-diffusion cellular automata [1]. A secure digital image communication scheme based on patterns evolving in a Beddington-DeAngelis-type predator-prey model with self- and cross-diffusion is proposed in [2]. Considerations on hardware implementation of image steganography based on reaction diffusion models are presented in [3]. SOP induced by evolutionary spatial 2×2 games are

exploited for hiding and transmitting secret visual information in [4]. Competitively and non-diffusively coupled non-linear maps are used for hiding secret visual information in [5].

However, above-mentioned pattern formation algorithms do exhibit a number of drawbacks in secret image communication applications. The self-organized pattern produced in a model of reaction-diffusion cellular automata [1] clearly resembles the initial fingerprint image and cannot be considered as an image hiding algorithm. At least 10,000 time forward iterations are required for the formation of an interpretable pattern produced by the reaction-diffusion model in [2,3]. The inversion of a single pixel in the initial random image does not result into any changes in the self-organized pattern produced by the communication algorithm proposed in [4]. Self-organized patterns produced by competitively and non-diffusively coupled non-linear maps [5] are originated by wave propagation in isotropic media, what predetermines a rather low complexity of the pattern structure.

The main objective of this paper is to develop a computationally effective visual communication scheme which could preserve the security of the communication, but minimize all previously-mentioned drawbacks. It is well known that patterns produced by the atrial fibrillation (AF) model are originated from complex rules of self-organization and wave propagation in anisotropic media. The ability to exploit this complex pattern formation phenomenon in a digital image communication scheme is the main goal of this paper.

Atrial muscle is comprised from myocytes that form the primal structure of the tissue. Observable patterns formed by myocytes are not regular and conform to complex self-organizing rules as proposed in [6,7]. Cells within this structure are coupled mainly by longitudinal (end-to-end) connections rather than latitudinal (side-by-side) connections thus resembling a cable-like signal transmission [6,8]. Conditions such as fibrosis and scarring processes can weaken and damage the connections [6], change and adjust the network of functioning cells [9,10].

The whole interaction of cells within the network can be modeled as proposed in [11]. Longitudinal (end-to-end) signals are always transmitted, whereas latitudinal (side-by-side) signals are transmitted only with a probability ν. This non-symmetrical coupling corresponds to the physical organization of cable-like transmissions. As a simplification, the structure can be presented as a flat entity because the wall of the atrial muscle is relatively thin [8].

This paper is organized as follows. The model of the system is presented in Section 2; the formation of SOP is discussed in Section 3. A communication scheme based on SOP in the AF model is presented in Section 4; the sensitivity of the proposed communication scheme to perturbations of its parameters is discussed in Section 5; Concluding remarks are given in the final section.

2. The Model of the System

The general idea of cable like transmissions is implemented on a discrete grid as follows. Three states of cells are considered: the resting state, the excited state and the refractory state. Resting cells and excited cells interact in two directions with different probabilities—probability 1 for the longitudinal direction and probability ν for the latitudinal (transversal) direction. Right after the cell is excited it enters the refractory state where it remains for the time period equal to τ (as illustrated in Figure 1).

In order to recreate some basic topological features of the atrial muscle periodic boundary conditions in the transversal direction can be combined with open boundary conditions in the longitudinal direction. This corresponds to the topology of a cylinder that is useful in order to investigate the effects of spontaneous heterogeneity that take place on the front of the propagating wave.

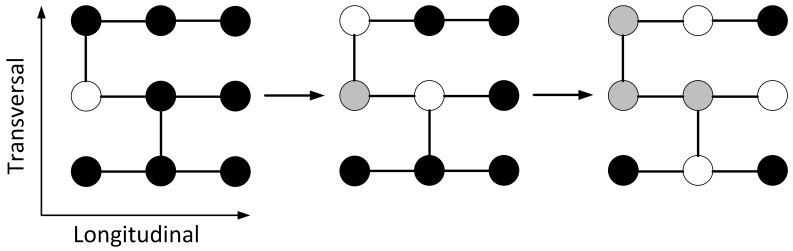

Figure 1. The diagram of interaction between cells within the network. Resting cells (black) and excited cells (white) interact in two directions with different probabilities. The resting cell becomes excited if it interacts with another excited cell. An excited cell (white) enters a refractory state (gray) for a time period τ.

In general, once the initial grid is fixed, all the interactions that can be numerically simulated depend only on system parameters ν (the probability of interactions along the transversal direction) and τ (the time spent in the refractory state).

However, the interactions between cells can be seriously complicated by dysfunctional cells. That can be illustrated by a simple computational experiment in Figure 2. Pacemaker cells are placed at the left boundary of the digital image and initiate the wave front which propagates to the right in all longitudinal cables (Figure 2a). However, because of dysfunctional cells, this is not always the only wave direction. The dysfunctional cell may block the propagation wave front (Figure 2b). The interplay between the wave fronts can form different patterns as shown in Figure 2c. Note that the boundary conditions are periodic.

Figure 2. Initial plane vertical wave is induced at left side by pacemaker cells (**a**). However, one cell is dysfunctional and blocks the propagation of the wave front (**b**). Due to the vertical connections between longitudinal cables, the resulting process forms a pattern (**c**).

However, such computational setup as illustrated in Figure 2 requires many time-forward interactions for the formation of a well-developed patterns. The wave front must propagate over all plane (and preferably more than once); it has to collide with all dysfunctional cells.

Let us consider an alternative computational setup where pacemaker cells are randomly distributed across 2D plane. Now, wave propagation continues to all directions and collide with each other. The benefit of such AF model implementation is that it requires less than 1% cells to be initially excited in order to form self-organized patterns (Figure 3).

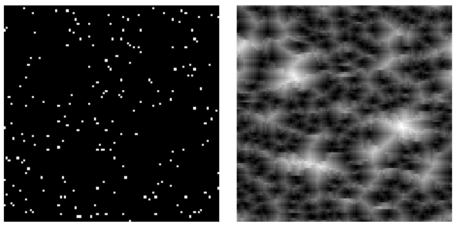

Figure 3. Initial cell state conditions (**a**) and the resulting pattern after 20 iterations (**b**). Parameter ν is set to 0.5; $\tau = 20$.

The computational efficiency of the numerical AF scheme can be enhanced even further by decreasing real pacing times τ of the cells. Optimal pacing time τ depends on the number of initially excited cells and the length of simulation. If τ is too small not all plane cells become excited, thus pattern is not fully formed. Otherwise, a too long refractory period results in relatively static pattern, because process cannot evaluate it is stuck in the same place.

3. Self-Organizing Patterns

3.1. Initial Conditions

Initial states of all cells are set as randomly uniformly distributed numbers over the real interval $[0; 1]$. Connections between cells in the transversal direction are distributed randomly as well. A pseudo-random number generator can be used for the reduction of the amount of information needed to define a unique configuration of the AF model. The benefit of such an approach is that a single seed of the random number generator defines all states and connections between cells.

For example, the chaotic Logistic map $a_{i+1} = 4a_i\,(1 - a_i)$ [12] can be used for the efficient generation of pseudo-random numbers. Every pseudo-random number generator has its drawbacks—the chaotic Logistic map has a limited uniformity of generated values, stable windows and relatively small space of valid seeds. The Logistic map can be enhanced and extended—alternative versions of the map such as an intertwined Logistic map [13] can eliminate some of these drawbacks. However, the standard Logistic map in also successfully used in various image encryption techniques and protocols [14,15]—we also continue computational experiments with the standard Logistic map.

Let us consider a regular grid with periodic boundary conditions. The chaotic logistic map with the initial value $a_0 = 0.02$ is used to generate a chaotic sequence; the generated discrete values of the sequence are sequentially assigned to every node on the grid (row by row). The resulting digital image is illustrated in Figure 4 (here 0 corresponds to black; 1—to white; all intermediate values—to appropriate grayscale levels).

Initial cell dichotomous states are now defined by a simple binary rule. A cell is set to be in the excited state if the value of the grid node is lower than δ; $0 < \delta \ll 1$. Thus, only $\delta \cdot 100\%$ cells would be excited in the initial state.

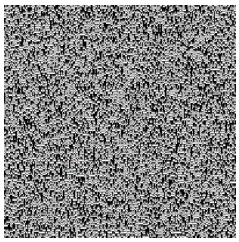

Figure 4. Pseudorandom initial conditions generated sequentially by the Logistic map; the initial value of the Logistic map a_0 is set to 0.02.

The same rule is used to generate the connection map—but the transversal connection probability ν is used instead of δ to describe transversal connections. In addition, different a_0 could be used in this Logistic map.

3.2. Parameters of the AF Model

The resulting SOP governed by the AF model depend on few parameters:

1. The cell excitation probability δ (in random initial conditions);
2. The connection map with corresponding probability of transversal connections ν;
3. Refractory period τ;
4. The number of time-forward iterations n.

Some of typical patterns are illustrated in Figure 5. It is clear that different connection maps result in the apparent effect of stretching—smaller values of ν result into more rhombus-like form of patterns; larger values of ν result in more horizontally stretched shapes (Figure 5a,b).

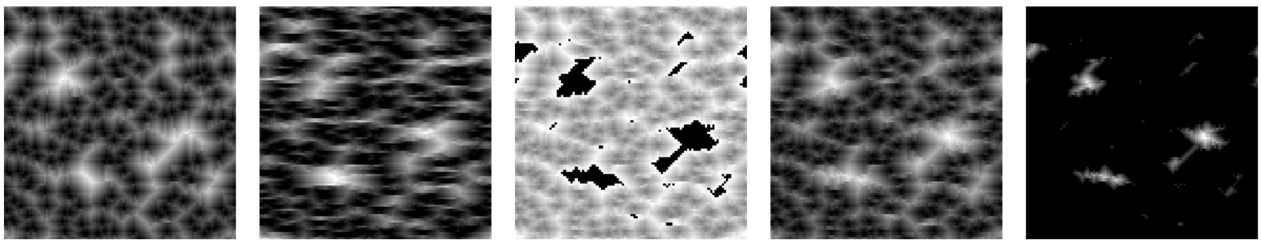

Figure 5. Comparison of self-organizing patterns (SOP) for different values of parameters. (**a**) $\nu = 0.1$, $\tau = 20$, $n = 20$, $\delta = 0.001$ (**b**) $\nu = 0.9$, $\tau = 20$, $n = 20$, $\delta = 0.001$ (**c**) $\nu = 0.5$, $\tau = 20$, $n = 10$, $\delta = 0.001$ (**d**) $\nu = 0.5$, $\tau = 20$, $n = 20$, $\delta = 0.001$ (**e**) $\nu = 0.5$, $\tau = 20$, $n = 30$, $\delta = 0.001$.

Another important parameter is the number of time-forward iterations n. It appears that a richest pattern is formed when n is close to the refractory period τ (Figure 5d). Only some of the cells are

excited in a small number of time-forward iterations (Figure 5c). Relatively large regions of cells remain unexcited. The boundaries of these black regions seem to be discontinuous due to the complexity of interactions between cells. All cells start converging to the resting state when the number of time-forward steps considerably exceeds the refractory index (Figure 5e).

Refractory period τ cannot be too short—a sufficient number of cells must be excited for the formation of an interpretable self-organized pattern. On the other hand, the number of initially excited cells is too high and the developed patterns are too scrambled if the probability δ is too large (Figure 6a). The formation of such a pattern does not require a long refractory period—however the pattern becomes static after a few iterations and then fades out altogether (Figure 6). Note that all patterns illustrated in Figure 6 are normalized to the full grayscale range—therefore some patterns appear brighter and some others—darker.

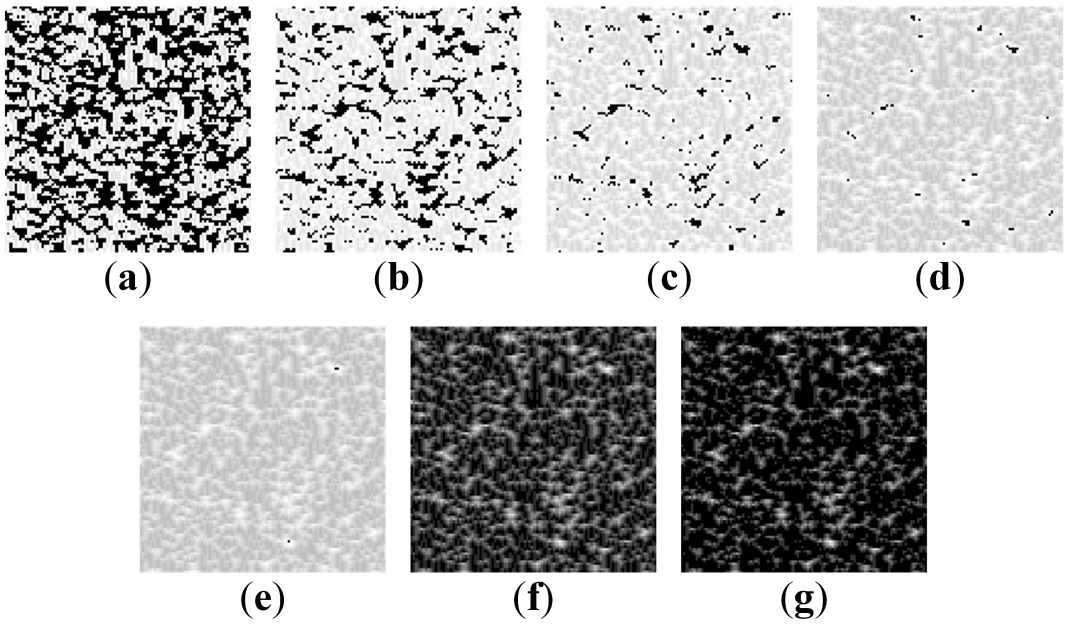

Figure 6. Iterative processes at $\nu = 0.5$, $\tau = 10$, $\delta = 0.1$. (**a**) $n = 1$ (**b**) $n = 2$ (**c**) $n = 3$ (**d**) $n = 4$ (**e**) $n = 5$ (**f**) $n = 6, 7, 8, 9, 10$ (**g**) $n = 11$.

The cell excitation probability δ is closely related to the number of iterations n (in terms of the richness of the pattern). In general, it is better to fix that number of iterations so that the formation of static images can be prevented. In this case best results are produced at $\tau = n$.

4. A Communication Scheme Based on Self-Organizing Patterns

As mentioned previously, SOP can be successfully employed to transmit secret visual information between the communicating parties. A typical communication scenario is presented in a scheme that consists of the following steps.

Initially, Sender and Receiver must use an asymmetric (arbitrary) protocol in order to determine the initial value a_0 and the number of time-forward iterations n (parameters ν, τ, δ, L_x, L_y must be predetermined beforehand).

1. Sender generates pseudo-random matrices of the initial cell excitation states and the connection map by using the Logistic map with the initial value a_0; the size of the matrix is set to $L_x \times L_y$; the parameters of the AF model are ν and δ. Initial random matrix is dichotomous (cells contain binary values 0 or 1); connection between cells are random.
2. Sender modifies the pseudo-random matrix of initial cell excitation states by inverting pixels corresponding to the dot-skeleton representation of the secret image.
3. Sender executes n time-forward iterations starting from the modified matrix of initial conditions and sends the image of the self-organized pattern to the Receiver.
4. Receiver generates the identical copy of pseudo-random matrices of initial cell excitation states and the connection map by using the chaotic Logistic map with the initial value a_0 and parameters of the AF model (ν and δ); the size of the matrix is $L_x \times L_y$ (this is an identical copy of the matrix generated by the Sender in Step 1).
5. Receiver executes n time-forward iterations starting from the non-modified initial conditions.
6. Finally, the difference between the digital images of the patterns produced by the non-modified and modified initial conditions reveals the secret.

Unfortunately, straightforward inversion of pixel values in the areas occupied by the secret image (in the digital image of initial conditions) does not work well in general (Figure 7). The "secret" image is shown in Figure 7a; the digital image representing initial conditions (with inverted pixels in the zones occupied by the secret information)—in Figure 7b. The self-organized pattern is illustrated in Figure 7c. It is clear that such pattern is not safe—a naked eye can detect the contours of the secret original image. The difference image is shown in Figure 7d; the binarized difference image—in Figure 7e. Thus, the image hiding scheme proposed in [4] cannot be used with the AF model. However, a single dot (1×1 pixel) inversions in the initial conditions are not interpretable in self-organized patterns (Figure 7)—thus the further image communication scheme is based on single pixel inversion strategy.

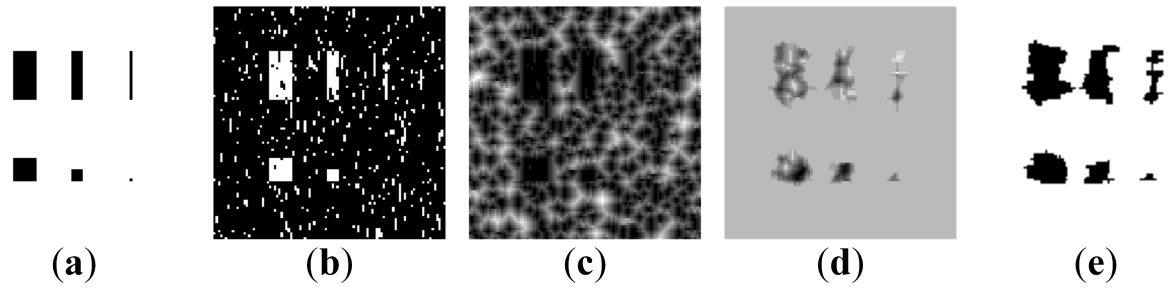

Figure 7. Big clusters of initially excited cells result in interpretable self-organized patterns ($\nu = 0.5$, $n = \tau = 20$, $\delta = 0.01$). (**a**) The secret image (**b**) Initially excited cells (shown in white) (**c**) The self-organized pattern (**d**) The difference image (**e**) The binarised initially excited cells.

A huge difference in the shape of the "secret" images can be seen between Figure 7a,e. It is clear that not all of the parameters considered in the SOP model (a_0, ν, δ) are equally applicable for the proposed communication scheme (even if an adequate formation of the self-organizing pattern is ensured). Firstly, the initial random background used for initial excitation should be close to

uniform (or homogeneous) in order to avoid empty spaces and larger initial cell clusters. Secondly, δ directly affects clearness of the resulting image (Figure 7c) as well as an easier interpretation of the difference image (Figure 7d). Meanwhile, probability ν does not have a big effect except stretching—however it is recommended to keep it in the range $(0, 1)$ and not use the trivial cases (0 or 1).

Let us consider four groups of a regular array dots (Figure 8a). Dots in four groups are respectively 15, 10, 5, 3 pixels away from each. Figure 8 illustrates difference images at different values of parameter δ. It can be seen that depending on the cell probability to be excited (parameter δ) the required minimum distance from dots (in the secret image) varies. Better information visibility of the decoded image is ensured by higher values of δ. However, denser initially exited cells lead to less resting cells—and this results in a less number of iterations required for a fully developed pattern. On the other hand, a smaller number of iterations results into smaller changes in the initial image.

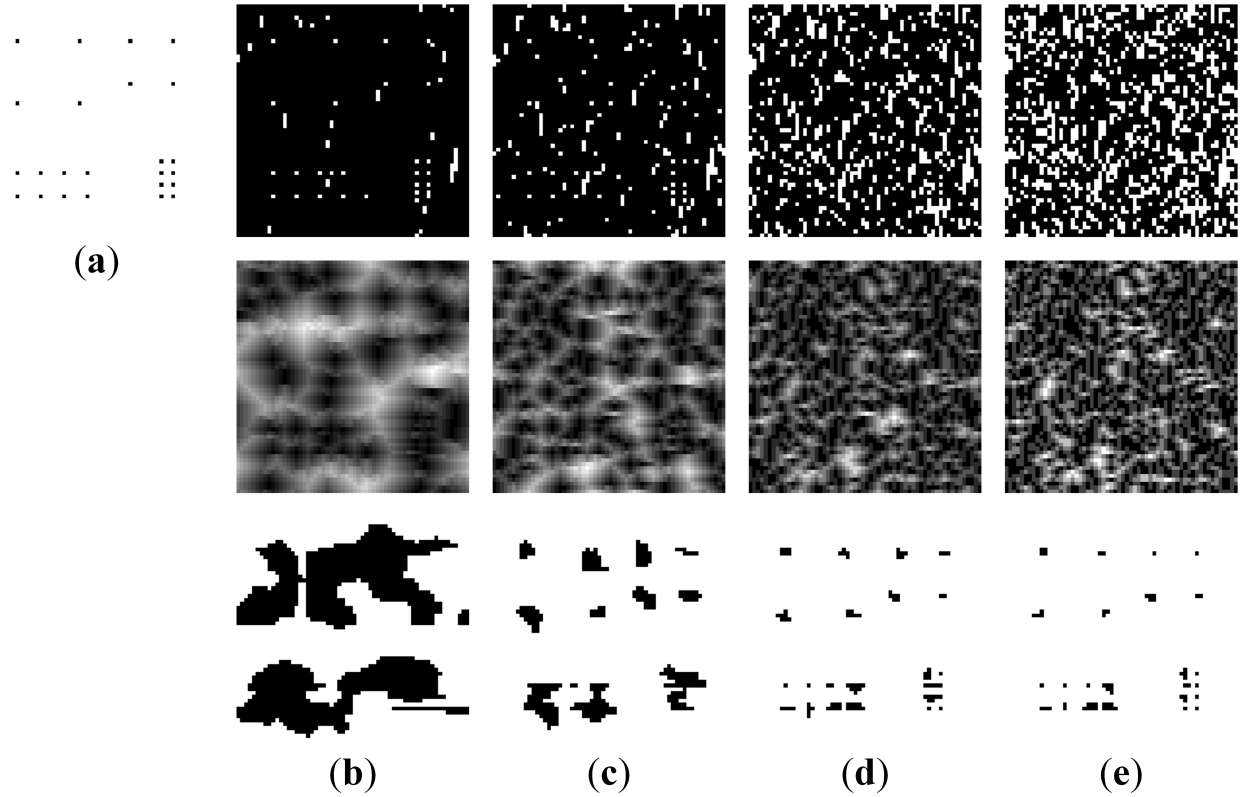

Figure 8. The initial dot-skeleton image (**a**) and SOP at different δ: the first row represents initial conditions; the second row—patterns; the third row—difference images. (**a**) $\delta = 0.001$ (**b**) $\delta = 0.01$ (**c**) $\delta = 0.1$ (**d**) $\delta = 0.2$.

The secret visual communication scheme based on SOP in the AF model can be illustrated in Figure 9 ($\nu = 0.2$, $\tau = n = 20$, $\delta = 0.08$). Before the transmission takes place, the original secret image is transformed into a dot-skeleton equivalent. The system parameters ν, τ, δ, L_x, L_y must be predetermined beforehand. Finally the pseudo-random number seed a_0 and the number of iterations n is transmitted by using the secure communications channels.

The original secret image is shown in Figure 9a. Its dot-skeleton equivalent is illustrated in Figure 9b. Using the parameter a_0 (as well as the parameter δ) the Sender generates the initially excited cells

(Figure 9c). The initial states of cells are inverted accordingly to the dot-skeleton representation (Figure 9d). The resulting self-organizing pattern is shown in Figure 9f. This pattern can be placed on top of a standard cover image (Figure 9e) by using the least significant bit (LSB) steganographic technique [16]. This is a standard spatial domain steganographic technique which manipulates LSB of pixels to embed the secret information into the cover image. The final cover image ready to be sent over to the Receiver via an open communication channel is shown in Figure 9g.

The Received obtains the cover image (Figure 9g) and reproduces the pattern (Figure 9f) by using a clean copy of the cover image (Figure 9e).

The remaining procedure for the Receiver is to simply re-generate the initial array of pseudo-randomly excited cells (as shown in Figure 9c) and to generate the pattern (the parameters of the AF model are privately known in advance)—the alternative pattern is illustrated in Figure 9h. Finally, the difference image between the two (Figure 9f,h) reveals the secret message as shown in Figure 9i.

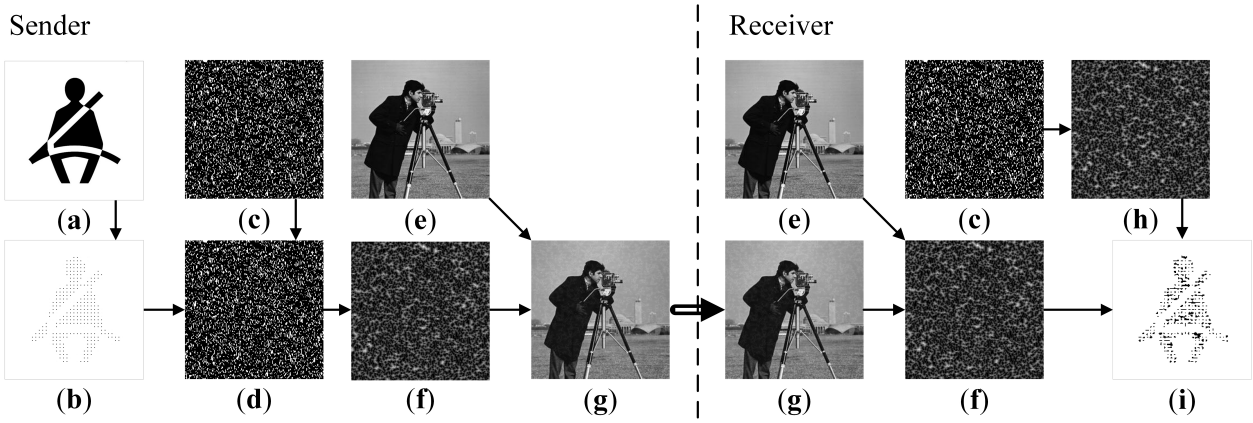

Figure 9. The flow chart diagram of the communication algorithm. Original image (**a**); dot-skeleton representation (**b**); initial conditions (**c**); perturbed initial conditions (**d**); cover image (**e**); perturbed self-organizing pattern (**f**); perturbed cover image (**g**); self-organizing pattern (**h**); difference image (**i**).

5. The Sensitivity of the Communication Scheme to Perturbations of System Parameters

The proposed communication scheme does work well with preselected set of system parameters. Slight changes in parameter values (when the Sender and the Receiver use different parameters) would compromise the communication system. Figure 10 illustrates the sensitivity of the communication system to perturbations; all illustrations represent difference images in the enhanced contrast mode. We set initial parameters to: $n = 20$, $\tau = 20$, $\nu = 0.2$, $\delta = 0.08$, $a_0^{ex} = 0.02$, $a_0^{con} = 0.02$, where a_0^{ex}—initial value of chaotic logistic map used to select initially excited cells, and a_0^{con}—for transversal connection map.

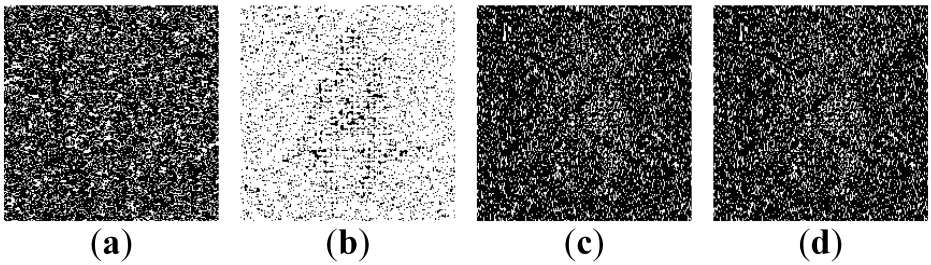

Figure 10. The sensitivity of the communication scheme to the perturbation of system's parameters. The difference images are shown when: (**a**) $a_0^{ex} = 0.021$ is used instead of 0.02; (**b**) $a_0^{con} = 0.021$ is used instead of 0.02; (**c**) $n = 21$ is used instead of 20; (**d**) $\tau = 19$ is used instead of 20.

The Sender uses all system's parameters as preset in the computational experiment illustrated in Figure 9—but the Receiver uses $a_0^{ex} = 0.021$ instead of $a_0^{ex} = 0.02$ (Figure 10a). The chaotic Logistic map is sensitive to small perturbations—thus it is natural to expect that the evolving patterns from different initial conditions would result into a different SOP image. Correct initial cell excitation map is essential in order to show the embedded secret (Figure 9a). However, AF model construction allows some perturbations in connection map (Figure 10b), thus different map does not completely brake the results and visual interpretation of the embedded secret is still possible.

Perturbations can be introduced in the number of iterations n and cell's refractory period τ. It can be noted that differences are only visible when $\tau < n$. Otherwise the model does not reach the breaking point when cells finish their relaxation period. As it can be seen in Figure 10c,d, changes by one time-step does hide most of the embedded image, but if the change is higher, the difference image does not reveal any secret.

6. Concluding Remarks

An image hiding scheme based on the atrial fibrillation model is presented in this paper. It appears that complex rules of self-organization and wave propagation in anisotropic AF media help to overcome such drawbacks of digital image communication schemes as long transients, relatively large primitives, the relative simplicity of the cover pattern. The secret image can be embedded into the spatially homogeneous dichotomous initial state by inverting the dot-skeleton representation of the secret, thus enabling an efficient and secure communication scheme based on SOP.

The SOP communication scheme can be used without LSB steganography. However, a transmitted SOP image may draw attention from eavesdroppers. LSB steganography could eliminate this threat. However, LSB steganography alone is prone to steganalysis algorithms. The SOP communication scheme ensures the security of the secret image even if LSB steganography would be compromised. Thus, the synergy of the SOP communication scheme and LSB steganography offers the added security to the transmitted image.

However, one should keep in mind that the presented AF model is a rough approximation of complex biological processes taking place in the tissue of the heart. Complex distribution of cardiac action potentials, spiral waves, arrhythmias, sinoatrial nodes and many other phenomena taking place in the

heart cannot be modeled using this AF model. Therefore, the extension of the presented communication scheme by introducing more complex interactions between cells is a natural objective of future research.

Acknowledgments

This research was funded by a grant (No. MIP-078/2015) from the Research Council of Lithuania.

Author Contributions

Martynas Vaidelys implemented the model and performed the experiments; Jurate Ragulskiene analyzed the simulation data, performed literature overview; Pranas Ziaukas adapted the AF model into the communication scheme; Minvydas Ragulskis proposed the idea, was supervising computational experiments and generalized the results.

Conflicts of Interest

The authors declare no conflict of interest.

References

1. Suzuki, Y.; Takayama, T.; Motoike, I.N.; Asai, T. Striped and spotted pattern generation on reaction-diffusion cellular automata—Theory and LSI implementation. *Int. J. Unconv. Comput.* **2007**, *3*, 1713–1719.
2. Saunoriene, L.; Ragulskis, M. Secure steganographic communication algorithm based on self-organizing patterns. *Phys. Rev. E* **2011**, *84*, 056213.
3. Ishimura, K.; Komuro, K.; Schmid, A.; Asai, T.; Motomura, M. Image steganography based on reaction diffusion models toward hardware implementation. *NOLTA* **2014**, *5*, 456–465.
4. Ziaukas, P.; Ragulskis, T.; Ragulskis, M. Communication scheme based on evolutionary spatial games. *Phys. A Stat. Mech. Appl.* **2014**, *403*, 177–188.
5. Vaidelys, M.; Ziaukas, P.; Ragulskis, M. Competitively coupled maps for hiding secret visual information. *Phys. A Stat. Mech. Appl.* **2016**, *443*, 91–97.
6. Luke, R.A.; Saffitz, J.E. Remodeling of ventricular conduction pathways in healed canine infarct border zones. *J. Clin. Investig.* **1991**, *87*, 1594–1602.
7. Verheule, S.; Wilson, E.; Everett, T.; Shanbhag, S.; Golden, C.; Olgin, J. Alterations in Atrial Electrophysiology and Tissue Structure in a Canine Model of Chronic Atrial Dilatation Due to Mitral Regurgitation. *Circulation* **2003**, *107*, 2615–2622.
8. Nakamura, K.; Funabashi, N.; Uehara, M.; Ueda, M.; Murayama, T.; Takaoka, H.; Komuro, I. Left atrial wall thickness in paroxysmal atrial fibrillation by multislice-CT is initial marker of structural remodeling and predictor of transition from paroxysmal to chronic form. *Int. J. Cardiol.* **2011**, *148*, 139–147.
9. Clayton, R.; Bernus, O.; Cherry, E.; Dierckx, H.; Fenton, F.; Mirabella, L.; Panfilov, A.; Sachse, F.; Seemann, G.; Zhang, H. Models of cardiac tissue electrophysiology: Progress, challenges and open questions. *Prog. Biophys. Mol. Biol.* **2011**, *104*, 22–48.

10. Clayton, R.H. Computational models of normal and abnormal action potential propagation in cardiac tissue: Linking experimental and clinical cardiology. *Physiol. Meas.* **2001**, *22*, R15–R34.
11. Christensen, K.; Manani, K.A.; Peters, N.S. Simple Model for Identifying Critical Regions in Atrial Fibrillation. *Phys. Rev. Lett.* **2015**, *114*, 028104.
12. May, R.M. Simple mathematical models with very complicated dynamics. *Nature* **1976**, *261*, 459–467.
13. Wang, X.; Luan, D. A novel image encryption algorithm using chaos and reversible cellular automata. *Commun. Nonlinear Sci. Numer. Simul.* **2013**, *18*, 3075–3085.
14. Pareek, N.; Patidar, V.; Sud, K. Image encryption using chaotic logistic map. *Image Vis. Comput.* **2006**, *24*, 926–934.
15. Kocarev, L.; Jakimoski, G. Logistic map as a block encryption algorithm. *Phys. Lett. A* **2001**, *289*, 199–206.
16. Fridrich, J.; Goljan, M.; Du, R. Reliable detection of LSB steganography in color and grayscale images. In Proceedings of the 2001 Workshop on Multimedia and Security, New Challenges, Ottawa, ON, Canada, 5 October 2001; pp. 27–30.

© 2015 by the authors; licensee MDPI, Basel, Switzerland. This article is an open access article distributed under the terms and conditions of the Creative Commons Attribution license (http://creativecommons.org/licenses/by/4.0/).